Needle flower-like ZnO-based chemiresistive sensor for efficient detection of formaldehyde vapors

Bidesh Mahata[1], Soumen Giri[2], Pallab Banerji[2] and Prasanta Kumar Guha[3]

[1]*School of Nano Science and Technology, Indian Institute of Technology Kharagpur, Kharagpur – 721302, India*

[2]*Materials Science Centre, Indian Institute of Technology Kharagpur, Kharagpur – 721302, India*

[3]*Electronics & Electrical Communication Engineering, Indian Institute of Technology Kharagpur, Kharagpur – 721302, India*

Abstract

The development of a chemiresistive sensor that uses needle-flower-like ZnO to effectively detect formaldehyde vapors is highlighted in the paper. The hydrothermal process at low temperature was used to prepare the sensing material. The morphological and structural characteristics of the synthesized material were assessed using X-ray diffraction (XRD) and field emission scanning electron microscopy (FESEM). Using a micropipette, the sensing material was transferred to the surface of the gold-based interdigitated electrodes to fabricate the device. The fabricated sensor was found to be more selective and sensitive to formaldehyde in the sensing study. The results showed an approximate response of 8 at 250 °C and 75 ppm formaldehyde. The lowest detection limit of the sensor was calculated as 480 ppb. The sensor has a great potential to monitor formaldehyde vapors in the indoor environment.

Keywords: ZnO, needle flower, chemiresistive, gas sensor, formaldehyde.

Address of correspondence
Dr. Prasanta Kumar Guha, Electronics & Electrical Communication Engineering, Indian Institute of Technology Kharagpur, Kharagpur – 721302, India

Email: pkguha@ece.iitkgp.ac.in

How to site this article
Bidesh Mahata, Soumen Giri, Pallab Banerji and Prasanta Kumar Guha., Needle flower-like ZnO-based chemiresistive sensor for efficient detection of formaldehyde vapors, J Cond. Matt. 2023; 01 (02):17-20

Available from:
https://doi.org/10.61343/jcm.v1i02.26

Introduction

Formaldehyde is a colorless, naturally occurring volatile organic compound (VOC) that is generally used as a preservative in the form of formalin (40% aqueous solution of formaldehyde) [1]. It is a by-product of the combustion of organic substances such as wildfire, vehicle exhaust, and tobacco smoke [2]. The source of the natural production of formaldehyde is the metabolism of α-amino acid serine in the living organism [3]. In industry, it is used to produce resins for coatings [4]. Recently, formaldehyde of high concentration (>5ppm) has been found in food items [5]. It is the most toxic indoor air pollutant with carcinogenic effects [6]. The sources of formaldehyde in indoor environments are paints, perfumes, adhesives, furniture, cosmetics, and preservatives [7]. It can cause fatigue, dizziness, respiratory problem, lung diseases, renal failure, coma, and even death [8,9]. The Occupational Safety and Health Administration (OSHA) sets an exposure limit of 0.75 ppm averaged over 8 h working period [10]. Therefore, it is vital to monitor formaldehyde concentration in an indoor environment efficiently.

There are standard techniques such as gas chromatography, liquid chromatography, ion chromatography, and spectroscopic techniques are available for accurately detecting formaldehyde [11,12]. But these are bulky, expensive, and lab-based techniques. Electrochemical sensors are costly and suffer from stability issues. In this contrast, the advantages of metal oxide-based chemiresistive sensors are low cost, small size, high sensitivity, fast response, high stability, easy interface electronics, and low maintenance [13]. ZnO is a versatile, eco-friendly n-type semiconductor material having a wide application range. In the field of gas sensors, ZnO nanostructures (rod, needle, flower, belt, particle, plate, etc.) were used due to their high surface area, durability, high sensitivity, fast response, and recovery [14]. The remaining scope of research is to address the selectivity issue.

In this work, a chemiresistive sensor was developed for efficient detection of formaldehyde employing well-defined needle flower-like ZnO material. The hydrothermal low-temperature approach was used to prepare the sensing material. Utilizing XRD and FESEM, the synthesized material's crystal structure and surface morphology were studied. The synthesized material was drop-cast onto ceramic substrate-based gold interdigitated electrodes (IDEs) to fabricate the sensor device. The sensing study of formaldehyde with the fabricated sensor device was performed in a custom-made gas sensing setup. The sensor exhibited a response of around 8 with 75 ppm formaldehyde present at 250 ºC. The theoretical limit of detection (LOD) of the developed sensor was calculated as 480 ppb. The sensor was sensitive and more selective towards formaldehyde among other VOCs such as 2-propanol, ethanol, and toluene. This study has significant implications for developing metal oxide-based, cost-effective, miniaturized, stable, sensitive, and selective formaldehyde detection.

Experimental Details

(a) **Chemicals used:** Zinc nitrate hexahydrate ($Zn(NO_3)_2$, $6H_2O$) and sodium hydroxide (NaOH) were obtained from Sigma Aldrich, MERCK. All the chemicals were utilized directly because of their high purity.

(b) **Synthesis process:** The sensing material was prepared through a hydrothermal route [15]. Using magnetic stirring (850 rpm), 0.31g $Zn(NO_3)_2$, $6H_2O$ was first dissolved in 25 mL of deionized (DI) water. Subsequently, the solution above was mixed with 1 M 15 mL of NaOH and stirred for 5 minutes. After that, the mixture solution was placed in an autoclave system and heated to 100 °C for five hours. After collecting the white precipitate, it was repeatedly cleaned with DI water and left to dry overnight at 60 °C. Finally, the calcination of the white powder was done at 450 °C for 90 minutes.

(c) **Device fabrication:** The gold IDEs with an alumina substrate base of dimension 5 mm × 6 mm and fingers of 90 µm width were used to fabricate the gas sensor device (Figure 1) by drop-casting the solution of the synthesized material over the IDEs. 1 mL of DI water was thoroughly mixed with 5 mg of the sensing material to prepare the solution. A micropipette was used to transfer precisely 10 µL of the aforementioned solution to the IDEs. Next, the device was dried for one hour at 60 °C.

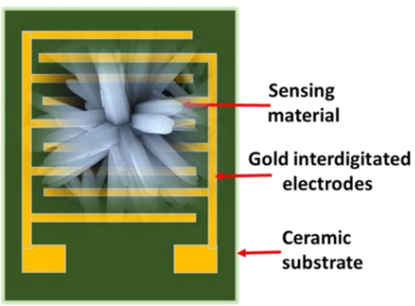

Figure 1: Schematic representation of the fabricated sensor device.

(d) **Gas sensing apparatus:** The sensing setup, which was based on a cylindrical chamber, was used to perform the sensing measurements. It comprised a hotplate, temperature sensor, mass flow controllers (MFCs), and semiconductor parameter analyzer. The fabricated sensor was stabilized at a particular temperature, and the sensing performance was studied in a dynamic manner with a constant 500 sccm airflow. The target VOCs were sent using a bubbler arrangement, and the response of the sensor was recorded. The formula for evaluating the sensor's response was Ig/Ia, where Ig and Ia were the saturated current with the exposure of target gas and air, respectively.

Results and Discussion

(a) **Morphological characterization:** The sensing material's morphology was examined using a Merlin FESEM. Figure 2a shows that a needle flower-like structure was formed. Each needle comprised six smooth surfaces and a sharp tip at the end. Needles were assembled together to form a flower-like structure. The structure facilitates more interaction sites for the adsorption of large number of analyte molecules.

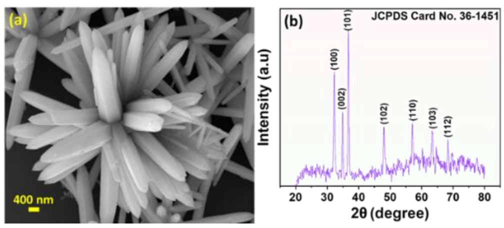

Figure 2. (a) FESEM image and, (b) XRD pattern of synthesized ZnO material.

(b) **Structural analysis:** The crystallographic study of the sensing material was investigated using a Bruker XRD characterization tool. The XRD pattern (Figure 2b) confirmed the crystalline nature and hexagonal phase of the sensing material with lattice parameters $a = b = 3.247$ Å, $c = 5.202$ Å, $\alpha = \beta = 90°$, and $\gamma = 120°$. The XRD pattern of the synthesized ZnO contained peaks at 2θ of 32.21º, 34.86º, 36.69º, 47.97º, 57.02º, 63.28º, and 68.36º corresponding to [100], [002], [101], [102], [110], [103], and [112] planes, respectively (JCPDS Card No. 36 - 1451). The average crystallite size of 27.7 nm was calculated from Scherrer's formula.

(c) **Formation and growth mechanism:** The nucleation and growth process explain the formation of needle-like structures. During hydrothermal conditions, $Zn(OH)_2$ nanoparticles were formed in an alkaline solution. The presence of OH^- ion accelerates the attachment and formation of $[Zn(OH)_4]^{2-}$ complex ion. Finally, it transforms into a needle-like structure due to rapid absorption and growth of OH^- ions on [0001] polar surfaces [15].

$$NaOH \rightarrow Na^+ + OH^- \quad \ldots(1)$$

$$Zn^{2+} + 2OH^- \rightarrow Zn(OH)_2 \quad \ldots(2)$$

$$Zn(OH)_2 + 2OH^- \rightarrow [Zn(OH)_4]^{2-} \quad \ldots(3)$$

$$[Zn(OH)_4]^{2-} \rightarrow ZnO + H_2O \quad \ldots(4)$$

(d) **Gas sensing study:** Initially, the sensor was stabilized at 5 V by passing a constant 500 sccm airflow. To determine the optimum temperature for the sensor, it was subjected to 75 parts per million formaldehyde over a temperature range of 150 to 300 °C (Figure 3a). The sensor's optimum temperature was discovered to be 250 °C. To obtain the transient response curve (Figure 3b), various formaldehyde concentrations between 15 and 75 ppm at 250 °C were passed through the sensing chamber. In the presence of 75 ppm formaldehyde, an 8 response was obtained. The selectivity test of the sensor was performed in the presence of other VOCs, such as 2-propanol, ethanol, and toluene (Figure 3c). The LOD was estimated from the following equation [16].

$$LOD = \frac{3\sigma_{noise}}{s}$$

where σ_{noise}= 1.28 $\times 10^{-8}$, is the standard deviation of noise and s=0.08, is the slope of the linear fitted (R-Square = 0.99) response vs. concentration graph (Figure 3d). The sensor's LOD was determined to be 480 ppb based on the evaluated values.

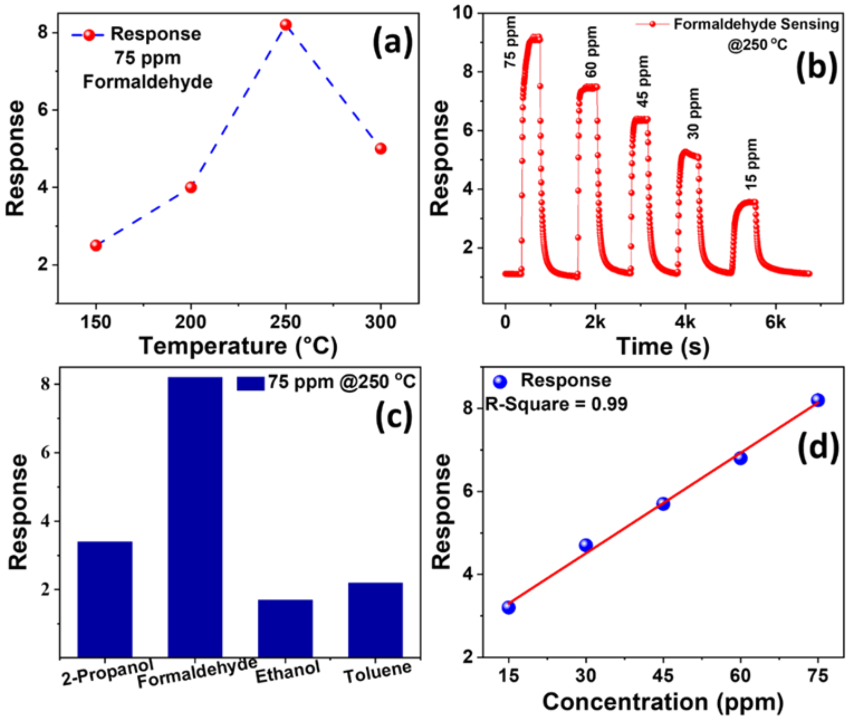

Figure 3. (a) Response vs. Temperature profile, (b) formaldehyde sensing performance, (c) selectivity test, and (d) response vs. concentration graph.

(e) **Gas sensing mechanism:** Analyte molecule surface adsorption and desorption are requirements for the sensing mechanism (Figure 4) [17]. Due to the strong electron affinity of oxygen molecules at 250 °C, the dominating oxygen species O^- adsorbed on the sensor layer's surface. As a consequence, at the grain boundary, the potential barrier height rises. Thus, the presence of air enhances the resistance of the material. The interaction between formaldehyde vapors and adsorbed oxygen molecules within the chamber results in the transfer of electrons to the conduction band of the sensing material. Therefore, during the existence of formaldehyde vapors, the potential barrier height and the resistance of the sensing material both drop.

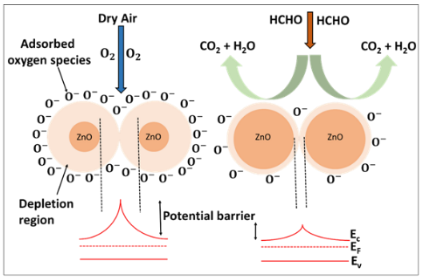

Figure 4. Schematic representation of formaldehyde sensing mechanism.

Conclusion

In this work, an efficient formaldehyde sensor was developed using needle flower-like ZnO material as a sensing layer. At low temperature, a hydrothermal process was used to synthesize the sensing material. XRD and

FESEM tools were used to characterize the synthesized material's morphology and structure. The sensor device was fabricated via a drop-casting method over the gold IDEs. The sensor device showed a higher response towards formaldehyde. At the optimum temperature and with 75 ppm formaldehyde vapors present, an 8 response was obtained. It was estimated that the sensor device's LOD was 480 ppb. Therefore, the proposed sensor can be utilized to detect formaldehyde vapors in the indoor environment.

Acknowledgement

The authors would like to thank the Indian Institute of Technology Kharagpur's Central Research Facility (CRF) for conducting the material characterization.

References

1. P. Wahed, M. A. Razzaq, S. Dharmapuri and M. Corrales, Food chemistry 202, 476-483 (2016).
2. Y. Huang, S. S. Ho, Y. Lu, R. Niu, L. Xu, J. Cao and S. Lee, in Molecules (2016), Vol. 21.
3. C. National Research, Review of the Formaldehyde Assessment in the National Toxicology Program 12th Report on Carcinogens. (The National Academies Press, Washington, DC, 2014).
4. A. Dorieh, M. Farajollah Pour, S. Ghafari Movahed, A. Pizzi, P. Pouresmaeel Selakjani, M. Valizadeh Kiamahalleh, H. Hatefnia, M. H. Shahavi and R. Aghaei, Progress in Organic Coatings 165, 106768 (2022).
5. U. N. Das, P. Jana, V. Dhanabalan and M. Xavier, Int J Curr Microbiol App Sci 7 (11), 2316-2322 (2018).
6. S. Dey, S. Santra, S. Sen, D. Burman, S. K. Ray and P. K. Guha, IEEE Sensors Journal 18 (14), 5656-5661 (2018).
7. J. Namieśnik, T. Górecki, B. Kozdroń-Zabiega ła and J. Łukasiak, Building and Environment 27 (3), 339-356 (1992).
8. B. Mahata, K. Dixit, S. Acharyya, P. Banerji and P. K. Guha, IEEE Sensors Letters 7 (8), 1-4 (2023).
9. K. C. Gupta, A. G. Ulsamer and P. W. Preuss, Environment International 8 (1-6), 349-358 (1982).
10. S. Acharyya and P. K. Guha, ACS Applied Electronic Materials 5 (6), 3446-3453 (2023).
11. M. Hunter, K. Bartle, P. Seakins and A. Lewis, Analytical Communications 36 (3), 101-104 (1999).
12. J. Schenk, D. D. Carlton, J. Smuts, J. Cochran, L. Shear, T. Hanna, D. Durham, C. Cooper and K. A. Schug, Environmental Science: Processes & Impacts 21 (2), 214-223 (2019).
13. G. Korotcenkov, Materials Science and Engineering: B 139 (1), 1-23 (2007).
14. S. Chaudhary, A. Umar, K. K. Bhasin and S. Baskoutas, in Materials (2018), Vol. 11.
15. S. Banerjee, P. Bhattacharyya and C. K. Ghosh, Applied Physics A 123 (10), 640 (2017).
16. S. Dey, S. Nag, S. Santra, S. K. Ray and P. K. Guha, Microsystems & Nanoengineering 6 (1), 35 (2020).
17. H. Ji, W. Zeng and Y. Li, Nanoscale 11 (47), 22664-22684 (2019).